ISSN 1330-3651 (Print), ISSN 1848-6339 (Online) https://doi.org/10.17559/TV-20220806010532
Original scientific paper

Tests on the Influence of Cyclic Loading and Temperature on the Behaviour of Flexible Pavement Reinforced by Geogrids with Numerical Simulation

Abdelkader MEDJDOUB, Mouloud ABDESSEMED*

Abstract: Crack growth is one of the most common failure modes in flexible linear infrastructure as a result of the effect of cyclic traffic loads and the climate influence. The results of an experimental study performed by applying different types of geogrids on asphalt concrete (AC) samples are presented in this paper. Static then cyclic loading are applied to these specimens reinforced before loading and the rest pre-cracked and loaded. Also, the influence of the type of geogrid, the type of loading, the frequency of cyclic loading and the variation of the ambient temperature were examined, by simulating the performance of real pavements in the great Algerian south, where the thermal gradient may reach the value of 30 °C. A total of 20 specimens were tested to evaluate the tensile strength, stresses and strains. A numerical analysis based on the finite element method, using an adapted software, was performed to match the experimental results found. The results (experimental and numerical) indicate that the optimal type and location of the geogrid, by static or cyclic loading, is critical to achieve stress and strain gains of up to 26% and thus can result in an aging delay of approximately five years compared to the application of traditional methods.

Keywords: asphalt concrete; cyclic/fatigue; experimental; geogrid; numerical analysis

1 INTRODUCTION

Linear infrastructures, such as roads and airport runways, are subjected to static and cyclic and sometimes dynamic loads and to the adverse effects of temperature as well, especially in hot climates. Sometimes, repetitive loads accelerate the onset of distress on the surface of the wearing course and/or in the depth of the pavement body (Fig. 1). In addition, stresses due to harsh environmental conditions, lead to several losses in structural pavements characteristics. Although owners regularly inspect runways and taxiways performing routine maintenance and/or emergency repairs, there is still a need to find adequate solutions to guarantee the safety of these infrastructures and restore their original mechanical characteristics [1, 2].

Figure 1 Rise and propagation of cracks on the road pavement

This can only be done when the pavement itself is excellently analyzed and diagnosed, in order to understand the types of distresses that have occurred and to find the finest solution to allow a good remedy to the problem [3-6]. Several strengthening techniques have been applied to flexible pavements in road and runway repairs over the last 30 years. In addition to the traditional techniques based on the application of asphalt concrete layer as overlay or the application of modified bitumen (MB) layers, or even high modulus asphalt concrete (HMAC), can significantly improve the mechanical properties of the pavement, but these methods remained mute in the case of the appearance and propagation of cracks on the pavement surface. Several authors have tried to explain the phenomenon of crack propagation, as apparent surface distresses, as well as the process of propagation of these cracks from a deteriorated layer to the pavement surface [7, 8]. In order to overcome these reflection cracks, different techniques have been developed in the past, the most important of which is the application of geosynthetic materials [9, 10]. It has been proven in many studies conducted in this field that the usage of geogrids (geosynthetic family) can delay the initiation of reflective cracks and reduce the propagation rate. Accordingly, it has been confirmed that for the strengthening and upgrading of degraded and cracked flexible pavements that have lost part of their mechanical characteristics, the application of these geogrids seems to become an alternative and effective repair solution [11, 12]. Eventually the performance of geogrids depends on the grid material, the shape of the mesh, the dimensions, the stiffness and the position in the section to be reinforced. Research has shown that these geogrids increase fatigue resistance, reduce degradation over time, reduce crack propagation and increase structural performance. Recent research, through laboratory investigations and in situ non-destructive testing, particularly in the road field, has highlighted the influence of these parameters [13]. However, at present, there is no consensus method for the design of pavements reinforced with geogrids. This is mainly due to the complexity of the mechanisms involved and the multiplicity of influencing parameters: cracking mechanisms (reflective, fatigue, thermal shrinkage, etc.), traffic, temperature, properties of the materials in place, properties of the rehabilitation materials, properties of the geogrid layer and, finally, the geogrid-asphalt interaction. The choice of the type and location of the geogrid is therefore mainly based on experience [14].

In this paper, we propose an experimental laboratory simulation performed on asphalt concrete (AC) specimens (slabs) reinforced with four different types of geogrids. Each type of geogrid was tested by tensile force to identify its mechanical characteristics in tension.

A total number of twenty (20) AC slabs, with or without reinforcement, were tested under cyclic loading

(called fatigue test) [15]. This was accomplished using these geogrid-reinforced bi-layer slabs and control slabs. The effect of temperature was considered by taking two cases: a temperature of 20 °C (corresponding to that in the northern part of Algeria) and 50 °C (which corresponds to the temperature of the arid climate in the south of Algeria). The objective of this study is to analyze the potential benefits of using geogrid reinforcement in a flexible pavement, such as the mitigation or delay of crack growth in the surface layers of linear infrastructure reinforcement. To this end, fatigue tests by the application of cyclic loads were carried out in the laboratory. In order to calibrate the experimental results found, a numerical work based on the finite element method, with adapted commercial software was carried out, determining the values of the deformation stresses, with the same assumptions of the experimental work in the laboratory.

Consequently, the apparent crack growth rate and the displacement at the base of the AC liner depended on the Young's modulus of the geogrid sheet used. Also, the value of this modulus (E), affects the vertical displacement of the AC liner and the number of load cycles before failure.

The difference found between the experimental and numerical results did not exceed 5% (stresses or strains) and the temperature had a detrimental effect on the mechanical performance of unreinforced asphalt pavements. However, these performances can be restored to their initial values during geogrids insertion, regardless of their type and position in the pavement body [16].

2 EXPERIMENTAL PROGRAM

2.1 Materials Used

For the preparation of the test specimens, a bituminous concrete of the studied composition, four (04) different types of geogrids and a bitumen emulsion were used. All these materials were selected due to the conditions of the tests, the available equipment and instrumentation in compliance with the current standards [17, 18].

2.1.1 Asphalt Concrete

The asphalt concrete used for the manufacture of the specimens was made according to the UNE-EN 13108-1 standard [19]. In order to determine the adequate dosage, a study of the formulation was made, with dosages of 5.7%, 6%, 6.3% and 6.6% of asphalt binder. The choice of these dosages was adopted, after several trial attempts. The materials used are: crushed sand (0/3), gravel (3/8), medium gravel (8/15) and 35/50 binder (used for road bitumen) [20]. Tab. 1 shows the studied composition of the mixture. The cylindrical specimens (101.6 × 63.5 mm), made for this purpose (for each dosage), gave better values for the stability measurement with the test "Marshal" [21], for the dosage of 5.7%, with a creep equal to 3.562, a quotient Marshal of 4.781 and a stability of 17.03 kN. Regarding the measurement of water sensitivity test "Duriez" on hydrocarbon mixtures, according to the standard "NA 5226/ NF P 98-251-1" [22], six specimens (of identical dimensions) of each dosage were tested with three immersed in water and three dry. The results found for this test are illustrated in Fig. 2, with the best value of the immersion ratio of 0.966 for the 5.7% dosage.

Table 1 Composition of the asphalt concrete dosage

Composition of the mixture / Dosage		Unit / %			
Asphalt binder	35/50	5.70	6.00	6.30	6.60
Sand	0/3	40	40	40	40
Gravel 1	3/8	42	42	42	42
Gravel 2	8/15	18	18	18	18

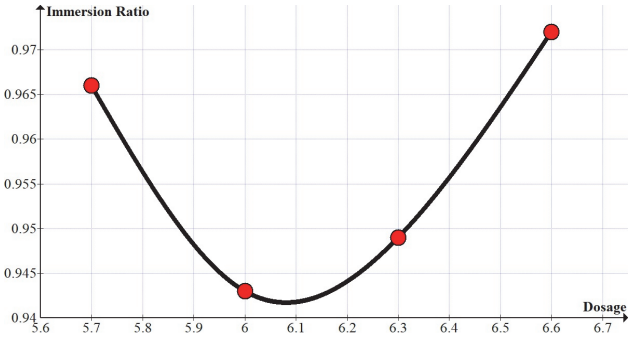

Figure 2 Immersion dosage ratio curve

2.2 Geogrids Layers

In order to determine the mechanical characteristics of each geogrid used, which is frequently called "quality control", two tests were carried out. The first test is that of traction of the wide strips and that, in accordance with the standard "ISO-10319" [23], using the universal traction machine "Instron 5900" (Fig. 3), located at the control center of public works (CTTP) in Algiers. The second test is used to determine the mass at the surface of geosynthetic layers, according to the standard: ISO-9864 [24].

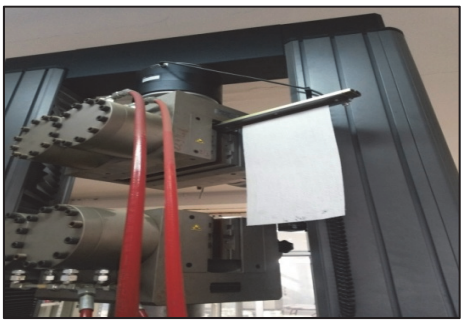

Figure 3 Instron 5900 Universal Machine

Different types of different geogrids were used, designated as G1, G2, G3 and G4, which are (Tab. 2):
- G1: Pre-coated woven-knitted-tramé geogrid (bitumen-coated), 40 × 40 mm^2 opening (Fig. 4a).
- G2: Polyester woven-knitted-trampled geogrid with polyvinyl chloride (PVC) coated fibers, 40 × 40 mm^2 opening (Fig. 4b).
- G3: Geogrid with a reticulated structure of glass fiber yarns, covered with polymers and a layer of pressure sensitive adhesive, opening of 25 × 25 mm^2 (Fig. 4c).
- G4: Geogrid with woven-knitted-tramé structure made of glass filaments, opening of 25 × 25 mm^2, lined with a geotextile fabric made of needle-punched polypropylene fibers (Fig. 4d).

The results obtained during the quality control of the geogrids are summarized in Tab. 3, which confirm those given by the technical sheets of the suppliers of the geosynthetic products [25, 26]. It was found that almost all

the resistance values in both directions are within the range of variation of the values obtained by the laboratory tests.

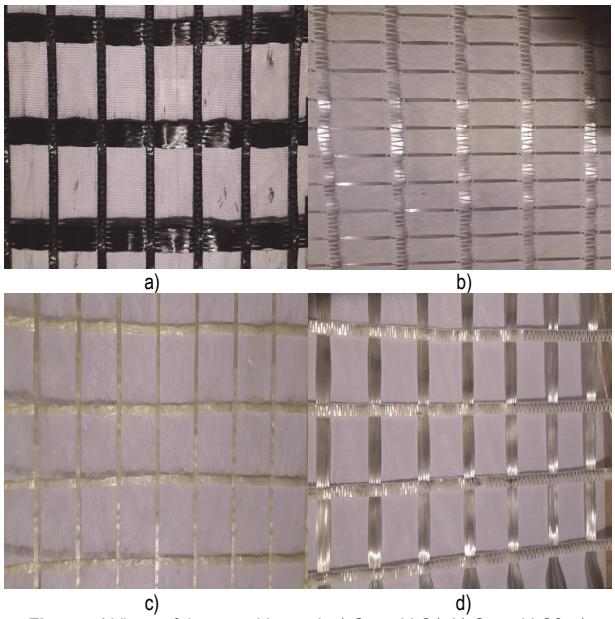

Figures 4 Views of the geogrids used: a) Geogrid G1, b) Geogrid G2, c) Geogrid G3, d) Geogrid G4

Table 2 Characteristics of the géogrids/reinforcement

Geogrid	Surface mass / gr/m²	Opening / mm²	Resistance breakage / kN/m	Tensile strain break	Bitumen emulsion / g/m²
G1	495	40 × 40	80	3%	500
G2	450	40 × 40	50	3%	500
G3	390	25 × 25	50	3%	500
G4	365	25 × 25	80	3%	1100

Table 3 Quality control test results for geogrids

Geogrid	Unit weight / kg/m²	$R_{traction}$ (longit.) / kN/m	$R_{traction}$ (trans.) / kN/m	Mesh / mm x mm	Hanging layer/ overdose / gramme
G1	452	78.9	81.7	40 × 40	500
G2	219	48.2	54.1	40 × 40	500
G3	375	50.9	54.3	30 × 30	300
G4	495	77.7	83.3	25 × 25	1100

In this study, a total of 20 specimens (slabs) were constructed consisting of two layers of asphalt concrete. The lower layer simulated an existing asphalt layer that was cracked, and the upper layer represented the reinforcement layer. Five different types of specimens were tested: first, the reference specimens (*R*) without reinforcement and then the four other geogrid-reinforced slabs previously tested. The first step in the manufacture of the slabs consisted of the production of a 50 mm high asphalt concrete layer in an appropriately sized mold and compacted using the rolling compaction procedure in accordance with the UNE-EN 12697-33 standard [27]. Then, a tack coat of bitumen emulsion was spread, the geogrid was placed in the freshly spread emulsion before breaking. Once the tack coat is broken, which can be visually observed by the change from an initial brown color (fresh emulsion) to a shiny black (residual bitumen film). The geogrid must be rolled out on the unbroken emulsion layer. In the next step, a 50 mm high bituminous layer was added on top of the first one and compacted following the standard mentioned above. The plan dimensions of each layer were (150 × 380 mm²). In order to simulate a road with cracks, a 40 mm notch was made at the base of the slab (10 mm below the geogrid) by sawing, in order to impose the location of the crack inception (Fig. 5).

For the mechanism of cracking and crack propagation, the application of a rolling load always causes a bending deformation of the pavement layers. This induces compressive stresses at the top and tensile stresses at the base of the asphalt layers. The accumulation of load cycles leads, beyond the limit, to the appearance of transverse and/or longitudinal cracks at the base of the asphalt structure which propagate towards the surface. This generates pavement fatigue, affecting the top layer (wearing course) or sometimes all the layers of the structure.

Thus, during the test, the propagation of the crack starts at the location of the pre-crack and in order to visualize, perfectly, the path of the crack, a layer of plaster was spread on the central zone of the samples.

Figure 5 Preparation of the mold for fatigue test

2.3 Test Description

The simulation designed in the laboratory, with the fabricated specimens, consists of the main elements representing a flexible pavement structure [28]:

- First layer of asphalt concrete (BB) with dimensions (380 × 150 × 50 mm).
- A geogrid layer, on top of the first layer of BB, with a tack coat of bitumen emulsion.
- The second layer of asphalt concrete of the exact dimensions as the first lay with light compaction to remove all air spaces.
- An elastic underlay in neoprene rubber with an elastic modulus of 10000 kN/m².

The test consisted of applying a controlled cyclic load of 5 kN amplitude (Fig. 6). This configuration was chosen in order to take into account the dynamic effect often produced on pavements by the traffic loads of heavy trucks [29]. The cyclic load was applied to the center of the slabs just above the crack through a circular loading plate (96 mm diameter). The period of application is 0.1 s, amidst a rest period lasting 0.05 s, in order to simulate high-speed truck traffic. The maximum amplitude load (5 kN) is applied to the specimen to create a pressure of 691 kPa above the specimen to simulate a wheel load from a 13 ton heavy truck (Fig. 7). This pressure has as much effect on the pavement structure as that of one million passenger vehicles [30]. In order to keep the slab and the loading plate in place during the dynamic loading, a minimum load of 0.2 kN was initially applied.

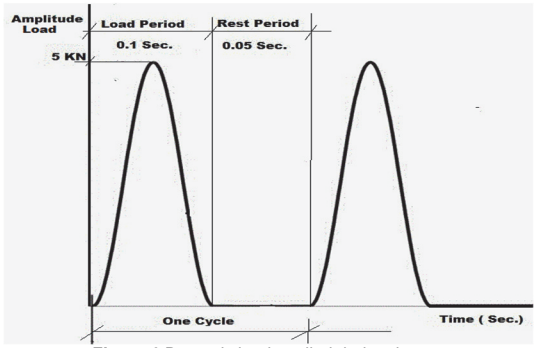

Figure 6 Dynamic load applied during the test

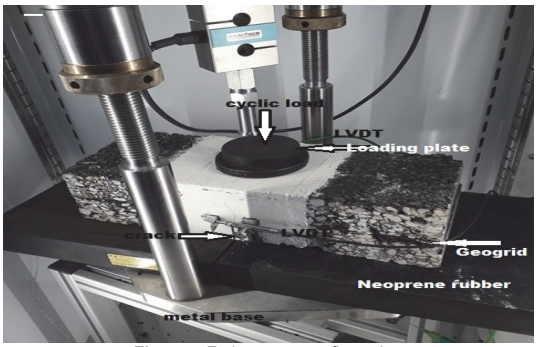

Figure 7 Fatigue test configuration

The dynamic test was performed by a universal testing machine (UTM-NU14) with servo-pneumatic drive and computerized autopilot system to control the load and the loading mode. It is equipped with a data acquisition system [31, 32]. The samples were tested at two different temperatures (20 °C and 50 °C), in a conditioned room for this purpose (Fig. 8). Before testing, it must be noted that all specimens were accommodated in a thermal chamber at the desired temperature for 16 h before testing. In order to obtain a good support for the slabs, a 50 mm thick rubber plate was placed between the metal base and the specimen. This neoprene rubber also has a role in holding the specimen in the initial position after the cyclic load is applied; the neoprene is split in two at the location of the induced crack in the specimen, thus facilitating the initiation and subsequent propagation of cracks. A dual measurement of the crack opening was recorded using two linear motion sensors (LVDTs) that were installed on both sides of the specimen at a distance of 10 mm above the interface. During the test, the crack opening was measured at different times, more frequently at the beginning of the test than at its end, when the crack growth was stabilized.

Figure 8 Equipment used for the measurements

2.4 Results and Discussion

The results obtained during the experimental investigation are displayed in Fig. 9, Fig. 10 and Fig. 11. Fig. 9 shows the effect of the number of loading cycles on the average crack opening, for an ambient temperature of 20 °C, for the five tests, which are: control slab (*R*), slabs G1, G2, G3 and G4, respectively reinforced by the four types of geogrids previously mentioned.

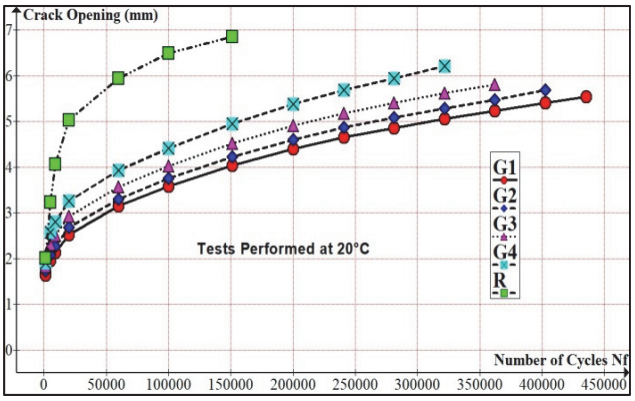

Figure 9 Evolution of crack openings as a function of the number of cycles (at 20 °C)

By applying a pre-crack of 1.6 mm, we notice at the outset of the test, the aperture of the crack is identical for all the samples. However, as the number of cycles (N_f) increases, the curves begin to take on different appearances, characterized by three stages: Stage1 with a rapid crack opening ($0 \leq N_f < 15000$), with an almost vertical linearity and a slight advantage for the reinforced slab (G1), where a gain of 66.7% compared to the specimen (*R*) is observed.

Stage 2, with a pseudo-linear phase ($15000 \leq N_f < 150\ 000$), the propagation of cracks increases, reaching 6.8 mm for specimen (*R*), 5 mm, 4.6 mm, 4.3 mm and 4 mm, for specimens (G4, G3, G2 and G1) respectively and the final phase, where a stop of crack propagation is observed. In this phase, the maximum openings of the cracks are: 6.8 mm, for only 150000 cycles (control slab *R*), 6.2 mm for 322000 cycles (slab G4), 5.7 mm for 370000 cycles (slab G3), 5.5 mm for 405000 cycles (slab G2) and 4.6 mm for 435000 cycles (slab G1) (Fig. 10).

Figure 10 Crack propagation of the G4 geogrid (50 °C)

For the tests at the temperature of 50 °C (Fig. 11), the same curves are obtained, concerning the evolution of the

average value of the crack opening as a function of the increase of the number of cycles (N_f), with a noticeable decrease of the number of loading cycles.

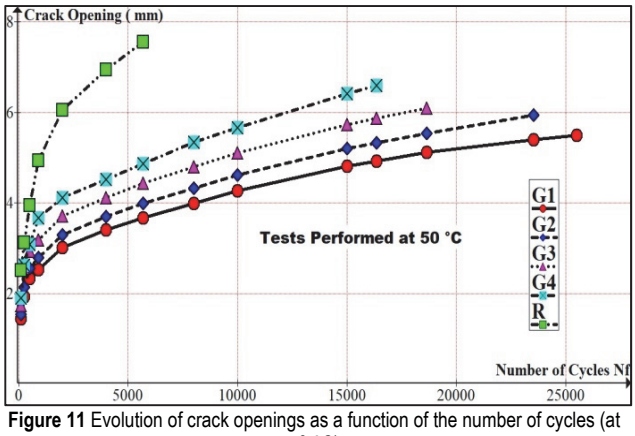

Figure 11 Evolution of crack openings as a function of the number of cycles (at 50 °C)

The curves begin to take different gaits, characterized by the three stages (as the ones at the temperature of 20 °C): Stage 1 with rapid crack opening ($0 \leq N_f < 1000$), with almost vertical linearity and a slight advantage (33.9% gain) for the reinforced dallet (G4). Stage 2, with a pseudo linear phase ($1000 \leq N_f < 4900$), the crack propagation increases, reaching 7.5 mm for the slab (*R*), 4.9 mm, 4.4 mm, 4 mm and 3.6 mm, respectively for the slabs G4, G3, G2 and G1 and the final phase, in which a stop of the crack propagation is observed In this phase, the maximum openings of the cracks are: 7.5 mm, for only a number of cycles of 4900 (control slab), 6.6 mm for 16000 cycles (slab G4), 6 mm for 19000 cycles (slab G3), 5.9 mm for 24500 cycles (slab G2) and 5.5 mm for 25900 cycles (slab G1).

The results obtained for the temperatures 20 °C and 50 °C, indicate that the number of cycles (at 20 °C) is 435000 for the slab with the most adapted geogrid (G1) while only 24500 for the same reinforced slab (G1) accompanied with the temperature of 50 °C, which gives an idea of the endurance of pavements reinforced by geogrid in a mild climate. The crack is strongly influenced by the opening caused, earlier than by the reinforcement by geogrid which reduces its propagation, only by 5.5 mm for the temperature of 50 °C and 4.6 mm for the temperature of 20 °C. Concerning the influence of the type of geogrid used in the reinforcement of the specimens, there is a clear difference between the curves representing the reinforced specimens and the curve of the control specimen "*R*", which indicates that all geogrids delay the rise of cracks and prolong the life of the reinforced pavement (increase in the number of cycles), but to different degrees [33, 34].

Indeed, the least efficient is the dallette (G4) which presents a larger crack opening than the G1, G2 and G3 geogrids. In addition, the anti-reflective behavior of the geogrids was analyzed using the crack opening value measured at the end of the test as a reference comparison value. For the percentages of reduction of the opening of the cracks (for the different geogrids compared to the reference sample), for the two ambient temperatures, there are significant differences between the results. In fact, for each geogrid, the reduction of the opening of the cracks, varies between values of 15% to 20% in the case of geogrids G1, G2 and G3 and a value of 9% for geogrid G4 for an ambient temperature of 20 °C. The G4 geocomposite has a different behavior, in fact, it has been noticed a low adhesion between the layers, and therefore, a poor performance as an anti-cracking system. On the contrary, apropos the case of samples with a geogrid like G1 and G2 in which there is a thin membrane that fuses with the bonding layer and integrates with the pavement, which offers a better resistance to the rise of cracks. Also, the slabs reinforced with G1 and G4 geogrids, that have a breaking strength of 80 kN/m, gave opposite results (fitter results for G1 and poor results for G4). Similarly, slabs reinforced with G1 and G4 geogrids, which have a tensile strength of 80 kN/m, showed contrasting results (fitter results for G1 and poor results for G4). While G2 and G3 geogrids with a lower tensile strength (50 kN/m), exhibited better results in the reduction of crack aperture, indicating that the tensile strength is an important, but not determining factor in the subsequent behavior of geogrids as anti-cracking systems. For the influence of temperature, it was found that the increase of the temperature leads to the decrease in the service life of all samples (clear decrease in the number of cycles). Nevertheless, the behavior and the choice of the type gives the same effects, remains the same and the most perforated (G1) at 20 °C remains as perforated as at 50 °C plus the behavior of the geogrids did not change. The G1 geogrid increased the life span by 288% at 20 °C while 450% at 50 °C and this remark remains valid for the other geogrids. At high temperature, an increase in crack opening between 13 and 25% is recorded for 50 °C yet only 9 to 19% for an ambient temperature of 20 °C.

3 NUMERICAL ANALYSIS

3.1 Model and Analysis Elements

A three-dimensional (3D) numerical modeling using the finite element method (FEM), was developed using adapted commercial software that is based on the input of geometric and mechanical characteristics of the experimental model and the inserted geogrid [35, 36]. Four types of elements were chosen to model the specimen (slab) section. These are the neoprene plates (or this is the neoprene plate) at the base (similar to an elastic soil), then the 1st layer of asphalt (bituminous concrete) placed at the bottom, the geogrid sheet and the 2nd layer placed on the geogrid. These elements were expressed in the software according to the criteria of the Mohr-Coulomb model. This model is used to model granular materials and loose agglomerates, whose material strength parameters that are assumed in the Mohr-Coulomb analysis, consist of density (d), bulk modulus of elasticity (K), shear modulus of elasticity (G), Poisson's ratio (ν), angle of friction) (φ), angle of friction (φ), angle of expansion (Ψ), and coefficient of cohesiveness (C) [37]. The element chosen for the geogrid is a one-dimensional linear elastic block element. The finite element model was validated via comparison with the results of the experimental study on a set of laboratory tests [38]. The geometry, the simulation of the support layer, as well as the propagation of the pre-cracking are similar to those of the experimental work developed (Fig. 12). For the application of the static load, as well as the dynamic analysis, a circular geometry was

taken as contact surface. Mesh and convergence analyses were performed by testing the different models.

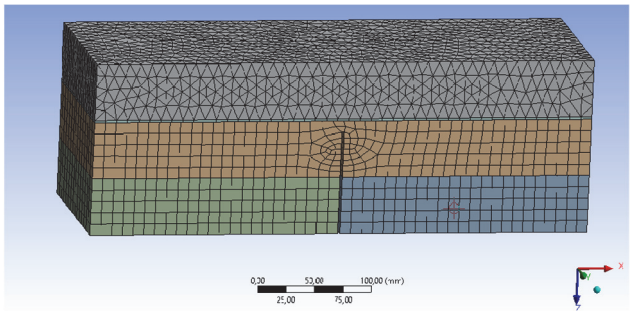

Figure 12 View of the mesh and pre-cracking

The mechanical properties of the four elements introduced in the model are represented in Tab. 4. Regarding for the densities, we took the values (for both temperature cases) of: 2790 (neoprene sheet), 2100 (old AC layer), 1100 (geogrid) and 2200 (AC reinforcement layer).

The modeling was done in order to compare the results found with those of the experimental campaign. We will take the following cases of figures: The modeling was performed in order to compare the results found with those of the experimental campaign. The following cases will be considered:

- Unreinforced pavement at a temperature of 20 °C in static and dynamic loading mode.
- Pavement reinforced with geogrid at a temperature of 20 °C in static and dynamic loading mode.
- Unreinforced pavement at a temperature of 50 °C in static and dynamic loading mode.
- Pavement reinforced with geogrid at a temperature of 50 °C in static and dynamic loading mode.

Table 4 Quality control test results for geogrids

Materials/ thickness / mm	Properties			
	Temperature at 20°C		Temperature at 50°C	
	Young Modulus E / Mpa	Poisson's ratio μ	Young Modulus E / Mpa	Poisson's ratio μ
Neoprene Plate / (50)	1100	0.49	1100	0.49
Old AC Layer / (50)	500	0.35	1030	0.45
Geogrid	800	0.30	800	0.45
Reinforced layer /(50)	7000	0.35	1200	0.45

3.2 Results of the Numerical Analysis

The results of the modeling are presented in the following figures. Hereunder are the displacements, stresses and strains, after reinforcement and according to the main axis of loading (static and dynamic). The values obtained indicate that the geogrids have prompted decrease of the displacements, vertical strains and stresses, when placed at the depth of the pavement. For the static loading (Fig. 13 to Fig. 18) at the temperature of 20 °C with placing the geogrid at 50 mm depth, the deformation is about 3.52 µm, while it decreases to 2.67 µm, a reduction of 32%. Concerning the displacement of the slab, we found a value of 0.01125 mm (before reinforcement) and 9.4 × 10^{-3} mm (after reinforcement), a reduction of 19%. This is also confirmed for the stresses, we found a gain of 14.3% (0.541 MPa before reinforcement and 0.473 after reinforcement). Thus, the choice of the best type of geogrid (G1) and the optimal placement of this geogrid, which is located at the bottom of the base layer (neoprene plate), yielded these positive results. Similar conclusions have been drawn by other previous researches, such as those of: Al-Azzawi [39], Correia [40] and Rahman [41], who studied the flexibility of flexible pavements using finite element modeling.

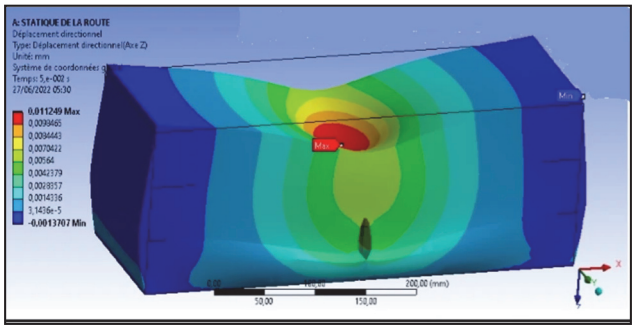

Figure 13 Vertical displacement (static load)

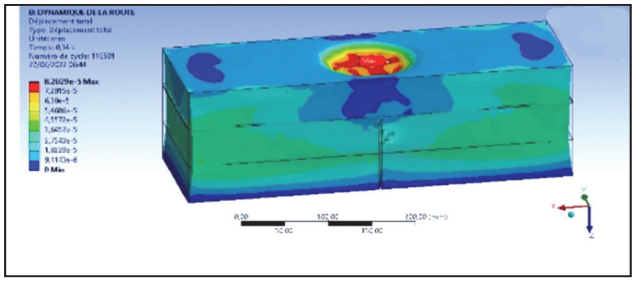

Figure 14 vertical displacements (dynamic load)

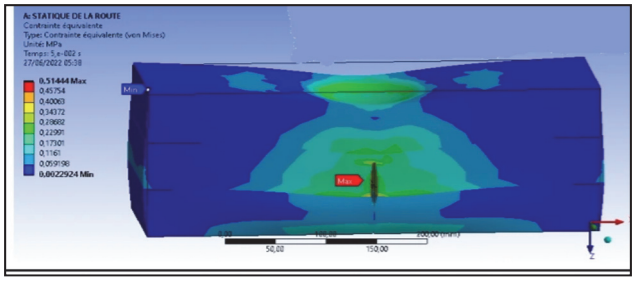

Figure 15 Stresses under static loading

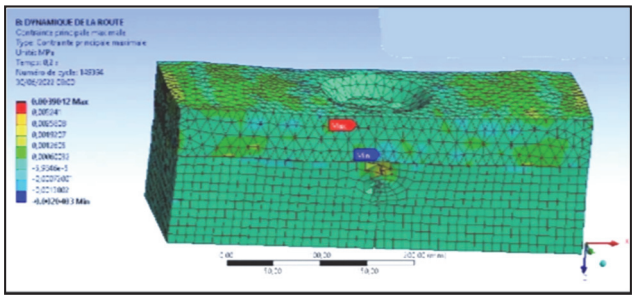

Figure 16 Stresses under dynamic loading

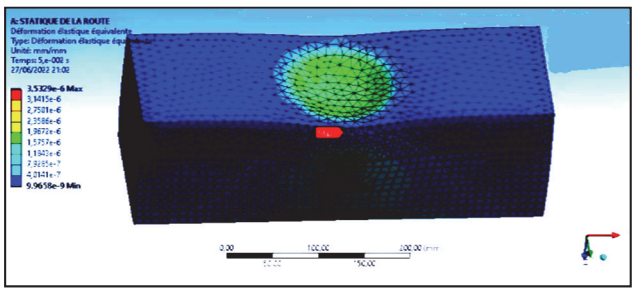

Figure 17 Deformations under static loading

The same conclusions are drawn by introducing the temperature of 50 °C, with reductions in the gains for strain (26% gain), displacement (13% gain) and stress (7.5% gain). The increase in temperature reduced the gain provided by the geogrid insertion advantage.

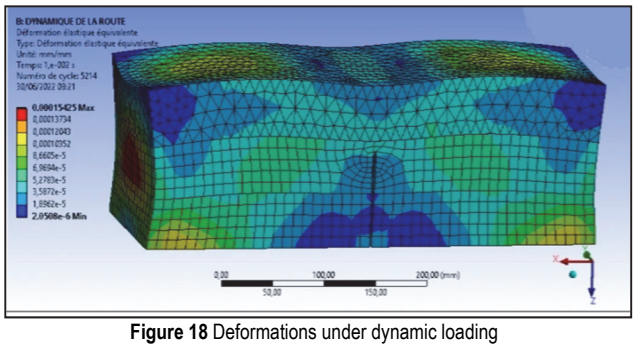

Figure 18 Deformations under dynamic loading

Numerically, for the dynamic loading (modal analysis) and simulating the cyclic load applied in the experiment, it is observed, examining the results previously established (Fig. 13 to Fig. 18), that the insertion of the geogrid, grants a gain for the behavior of the reinforced pavement and that the type of loading influences the values of displacements, deformations and stresses, at the points of application of the loads on the pavement. This is confirmed for the deformation, of value 154 µm, for the dynamic case and only 3.52 µm for the static case.

In fact, for both loading (static and dynamic) and the simulation of the cyclic load applied in the experiment, the results showed that the maximum value is just above the crack (at the level of the geogrid) at the base of the reinforcement layer. This tensile deformation must be taken by the geogrid, when it reaches a certain compatible level with the elongation limit of the geogrid. It is also found that the maximum deformations are occupying the vicinity of the crack, which creates microcracks that develop into longitudinal and transverse cracks that, in turn, rise to the surface. It can be seen that for the dynamic simulation for a sample without geogrid (Fig. 17), the value is greater than that of the static state with geogrid (154 µm), which indicates that the reinforcement by geogrid reduces the deformation in a very significant way, 44 times favorable for the dynamic case than the static case.

The displacement is reduced from 0.01125 mm (for the static case) to 8.263×10^{-3} mm (for the dynamic case). Finally, the stress undergoes a decrease during the dynamic loading and obtains a value of 0.0639 MPa opposed 0.5144 MPa for the static case. It is also noted that the temperature, whether for dynamic or static loading, has the same direct influence on the longevity (service life) of pavements. This was confirmed by the work of Abu El-Maaty [42].

3.3 Experimental Numerical Comparison

The comparison made between the experimental and numerical values found, for the case of the pavement, composed of two layers of asphalt and a base layer, with insertion of a layer of geogrid (4 different types) and which was simulated at an asphalt slab (AC) for the 3D finite element model using a convenient finite element software, has shown that the difference between the predicted numerical values and the experimental results found, did not exceed 5%, which can be more improved (smaller difference), in the case of nonlinear behavior of materials used [43]. Considering the choice of the model, the type of static and cyclic loading (fatigue) along with the assumptions of the linear behavior of the materials of the pavement layers, the measurement of deflections, displacements and stresses, as well as the service life in number of cycles, was well achieved numerically. A numerical reading (comparison between the experimental and numerical), shows that the number of cycles increases by 3.23% for the unreinforced specimen (at 20 °C) and by 1.23% for the reinforced one at the same temperature, in favor of the experimental result. Similarly, this number of cycles increases by 4. 84% for the unreinforced specimen (at 50 °C) and by 3.16% for the one reinforced by geogrid at the same temperature. Moreover, the number of cycles (numerically or experimentally), increases, in case of reinforcement, by 288% (at 20 °C) and 450% (at 50 °C).

The values found show that the geogrid (regardless of the type), with an optimal location, increases the life (the number of cycles increases) furthermore the increase of the temperature (arid areas), can play a deleterious role and reduce the life of the wearing course and consequently that of the pavement life as well. The table below (Tab. 5) displays all the values found concerning the number of cycles, in both cases of unreinforced and reinforced specimens with the optimal G1 geogrid.

It can be seen that the geogrid increased the fatigue life by about 3 times at the temperature of 20 °C and by 5 times at 50 °C. This is confirmed by the work of Chang et al. in 1999 [44] and Akrma et al. in 2022 [45].

Table 5 Experimental-numerical comparison

Designation	Lifetime (Number of cycles)		Gap
	Results experimental	Numerical results	%
Unreinforced specimen (at 20 °C)	151476	146394	3.23
Reinforced specimen with geogrid (at 20 °C)	435466	428476	1.63
Unreinforced specimen (at 50 °C)	5676	5414	4. 84
Reinforced specimen with geogrid (at 50 °C)	25494	24715	3.16

4 CONCLUSIONS

The anti-cracking behavior of the four different geogrids was studied experimentally using a new (modern or recently developed) test (sustained bending) under cyclic fatigue loading. The study examined the effects of geogrid type, tensile strength and the effect of temperature variation on crack growth. The validation of the experimental results was carefully performed by numerical modeling using the finite element method. Based on the results of this study, the following can be concluded:

- In almost all tests, inserting a geogrid over a cracked layer and then placing a new reinforcement layer delayed crack growth. In addition, the crack opening is further reduced with proper selection of the geogrid type.
- The choice of the most optimal position and the type of geogrid are critical variables, which influence the global behavior of the tested specimen and therefore, in order to

avoid a bad adhesion between the old and the new layer, a good implementation and an adequate choice of the emulsion layer are necessary.

- The inclusion of geogrids in reinforced pavements leads to a significant increase in the mechanical performance of the pavement. Samples with incorporated geogrids outperformed unreinforced samples in terms of resistance to cracking (by 20 - 27%) and an increase in service life of up to 450% (extended by about 5 times).
- The elevated temperature causes a decrease in the lifetime of all samples, however, the reinforced samples have the longest life span, which can go out 3 to 5 times compared to the control sample. In addition, the elevated temperature causes a greater opening of the cracks.
- The numerical analysis by the finites elements method (FEM) proved that the chosen model is in perfect concurrence with the reality of the tested sample. Variations in deviation of 3 to 5% are still excellent besides, this deviation can be reduced in case of the choice of the non-linear behavior of the used materials (asphalt concrete, base layer, etc.).
- It is possible to generalize this type of work to other problems and applications (airfield runway, road), whether in flexible or rigid pavement and can be very beneficial for the economy of the modernization projects.

Acknowledgements

The authors would like to thank all those who have contributed (or helped), directly or indirectly, to the realization of this work, in particular the executives of the laboratory of public works of the south LTPSud (Ghardaia), engineers and executives of the center of calculation of public works (CTTP) for having facilitated the task to the various tests carried out. Our sincere thanks to Pr Kenai Said, Director of the laboratory (LGMGC) at the University of Blida1. A great encouragement to Miss Abdessemed A.N.H, for her contribution in verification of the translation and for the form of the paragraphs of the paper. The principals and executives of the companies Afitex/Algerie and SarlChimiBat, find here our most sincere respects for their contribution and the provision of their products of geosynthetics.

5 REFERENCES

[1] Persia, L., Shingo Usami, D., De Simone, F., De La Beaumelle, V. F., Yannis, G., Laiou, A., Han, S., Machata, K., Pennisi, L., Marchesini, P., & Salathè, M. (2016). Management of road infrastructure safety. *Transportation Research Procedia*, *14*, 3436-3445. https://doi.org/10.1016/j.trpro.2016.05.303

[2] Solonenko, I. (2019). The use of cement concrete pavement for roads depending on climatic conditions. *Technical Gazette*, *13*(3), 235-240. https://doi.org/10.31803/tg-20190518181647

[3] Oliveira, H. & Correia, P. L. (2013). Automatic Road Crack Detection and Characterization. *IEEE Transactions on Intelligent Transporation Systems*, *14*(1), 155-168. https://doi.org/10.1109/TITS.2012.2208630

[4] Zumrawi, M. M. E. (2015). Survey and Evaluation of flexible Pavement Failures. *International Journal of Science and Research (IJSR)*, *4*(1), 1602-1607.

[5] Abdessemed, M., Kenai, S., & Bali. A. (2015). Experimental and numerical analysis of the behavior of an airport pavement reinforced by geogrids, *Construction and Building Materials*, *94*, 547-554. https://doi.org/10.1016/j.conbuildmat.2015.07.037

[6] Putra Jaya, R. (2021). A Comprehensive Review of Flexible Pavement Failures, Improvement Methods and its Disadvantages. *Key Engineering Materials*, *879*, 136-148. https://doi. org/10.4028/www.scientific.net/KEM.879.136

[7] Tjan, A. (1996). *Crack propagation modeling in flexible pavement structures*. Arizona State University ProQuest Dissertations Publishing, 9624835.

[8] Seslija, M., Radovic, N., Jeftenic, G., Starcev-Ćurcin, A., Pesko, I., & Kolakovic, S. (2020). The Influence of Temperature Changes on Concrete Pavement, *Technical Gazette*, *27*(6), 1990-2000. https://doi.org/10.17559/TV-20190222101126

[9] Suo, Z. & Gun, W. W. (2009), Analysis of fatigue crack growth behavior in asphalt concrete material in wearing course. *Construction and Building Materials*, *23*(1), 462-468. https://doi.org/10.1016/j.conbuildmat.2007.10.025

[10] Prieto, J. N., Gallego, I. J., & Pe´rez, I. (2007). Application of the wheel reflective cracking test for assessing geosynthetics in anti-reflection pavement cracking systems. *Geo synthetics International*, *14*(5), 287-297. https://doi.org/10.1680/gein.2007.14.5.287

[11] Moghadas, N. F., Noory, A., Toolabi, S., & Fallah, S. (2015). Effect of using geosynthetics on reflective crack prevention. *International Journal of Pavement Engineering*, *16*(6), 477-487. https://doi.org/10.1080/10298436.2014.943128

[12] Siriwardane, H., Gondle, R., & Kutuk, B. (2010). Analysis of flexible pavements reinforced with geogrids. *Geotechnical and Geological Engineering*, *28*(3), 287-297. https://doi.org/10.1007/s10706-008-9241-0

[13] Ferrotti, G., Canestrari, F., Virgili, A., & Grilli, A. (2011). A strategic laboratory approach for the performance investigation of geogrids in flexible pavements. *Construction and Building Materials*, *25*(5), 2343-2348. https://doi:10.1016/j.conbuildmat.2010.11.032

[14] Alimohammadi, H., Zheng, J., Schaefer, V. R., Siekmeier, J., & Velasquez, R. (2021). Evaluation of geogrid reinforcement of flexible pavement performance: A review of large-scale laboratory studies. *Transportation Geotechnics*, *27*. https://doi.org/10.1016/j.trgeo.2020.100471

[15] Abdessemed, M., Bazzine, R., & Kenai, S. (2021). Application of the Synthetics Geo-Composites in the Arid Zones for Rehabilitation of the Flexible Pavements Road Experimental Analysis. *Proceedings of the RILEM International Symposium on Bituminous Materials*, *27*, 279-284. https://doi.org/10.1007/978-3-030-46455-4_35

[16] Lee, S. J. (2008). Mechanical performance and crack retardation study of a fiberglass-grid-reinforced asphalt concrete system. *Canadian Journal of Civil Engineering*, *35*(10), 1042-1049. https://doi.org/10.1139/L08-049

[17] Kuan, H., Lee, H. J, Zi, G., & Mun, S. (2009). Application of Generalized *J*-Integral to Crack Propagation Modeling of Asphalt Concrete Under Repeated Loading. *Transportation Research Record: Journal of the Transportation Research Board*, *2127*(1), 72-81. https://doi.org/10.3141/2127-09

[18] Ahmed Alkawaaz, N. G., AL-Badran, Y. M., & Muttashar, Y. H. (2017). Evaluation of Geogrid- Reinforced Flexible Pavement System Based on Soft Subgrade Soils Under Cyclic Loading. *Civil and Environmental Research*, *9*(12), 55-68.

[19] Afnor Editions- Normes NF EN 13108-1 (2008). Mélanges bitumineux - Spécifications des matériaux Partie 1: enrobés bitumineux, 53 pages. Indice de classement: P 98-819-1, ICS: 93.080.20, France.

[20] Total Marketing Services, Fiche de données de sécurité (2018). Bitume routier 35/50, FDS n: 081641, 14, 92800 Puteaux, France.

[21] Tapkin, S., Cevik, A., & Usar, U. (2010). Prediction of Marshall test results for polypropylene modified dense bituminous mixtures using neural networks. *Expert Systems with Applications*, *37*(6), 4660-4670. https://doi.org/10.1016/j.eswa.2009.12.042

[22] Afnor Editions-Normes NF P98-251-1 (2002). Essais relatifs aux chaussées - Essais statiques sur mélanges hydrocarbonés Partie 1: essai DURIEZ sur mélanges hydrocarbonés à chaud, 12, Indice de classement: P98-251-1, France.

[23] Norme ISO 10319 (2015). Géo-synthétiques-Essai de traction des bandes larges, Edition 3, 14 pages, Comité technique ISO/TC 221, *Produits géo-synthétiques, ICS 59 080 70*, Géotextiles.

[24] Normes ISO 9864 (2005). Géosynthétiques-Méthode d'essai pour la détermination de la masse surfacique des géotextiles et produits apparentés, Comité technique, ISO/TC 221, Produits géosynthétiques, ICS 59.080.70, Geotextiles, 02.

[25] Afitex Algeria (in French) (2021). Production unit, rocessing of non-metallic minerals, wood and corkn Kharouba, Boumerdes, Algeria.

[26] Chemibat Algeria (in French) (2021). Import and supply of construction equipment, Hydra, Algeria.

[27] Afnor Editions- Normes NF EN 12697-34 (2020). Mélanges bitumineux - Méthodes d'essai pour mélange hydrocarboné à chaud - Partie 34 : essai Marshall, 13, Indice de classement: P 98-818-34, ICS: 75.140; 93.080.20, France.

[28] Ferrotti, F., Canestrari, A., & Grilli, A. (2011). A strategic laboratory approach for the performance investigation of geogrids in flexible pavements. *Construction and Building Materials*, *25*(5), 2343-2348. https://doi. org/10.1016/j.conbuildmat.2010.11.032

[29] Vale, C. (2008). Influence of vertical load models on flexible pavement response an investigation. *International Journal of Pavement Engineering*, *9*(4), 247-255. http://doi.org/10.1080/10298430701444977

[30] Bordes, P., Guinard, G., & Laurent, G. (1996). Routine pavement maintenance- A pratical guide (in french). *Service d'Etudes Techniques des Routes de Autoroutes (SETRA)*, 119.

[31] Arsenie, I. M., Chazallon, C., Duchez, J. L., & Hornych, P. (2017). Laboratory characterisation of the fatigue behaviour of a glass fibre grid-reinforced asphalt concrete using 4PB tests. *Road Materials and Pavement Design*, *18*(1), 168-180. https://doi.org/10.1080/14680629.2016.1163280

[32] Lau, C. K., Chegenizadeh, A., Htut, T. N. S., & Kikraz, H. (2022). Performance of the Steel Fibre Reinforced Rigid Concrete Pavement in Fatigue, *Building*, *10*(10). https://doi. org/10.3390/buildings10100186

[33] Rajagopal, K., Chandramouli, S., Parayil, A.. & Iniyan, K. (2014). Studies on geosynthetic-reinforced road pavement structures. *International Journal of Geotechnical Engineering*, *8*(3), 287-298. https://doi.org/10.1179/1939787914Y.000000004

[34] Ibrahim, E. M., El Badawy, S. M., Ibrahim, M. H. Gabr, A., & Azam, A. (2017). Effect of geogrid reinforcement on flexible pavements. *Innovative Infrastructure Solutions*, *2*(54), 1-15. https://doi.org/10.1007/s41062-017-0102-7

[35] Majumder, S. & Saha, S. (2021). Experimental and numerical investigation on cyclic behaviour of RC beam column joints reinforced with geogrid material. *Materials Today Proceedings*, *38*(5), 2316-2324. https://doi.org/10.1016/j.matpr.2020.06.415

[36] Ouadah, N., Abdessemed, M., &Kechouane, F. (2022). Dynamic behavior of concrete structures reinforced with nanotubes modified composites. *Romanian Journal of Materials*, *52*(1), 26-37.

[37] Al-Jumaili, M. A. (2016). Finite Element Modelling of Asphalt Concrete Pavement Reinforced with Geogrid by Using 3-D Plaxis Software. *International Journal of Materials Chemistry and Physics*, *2*(2), 62-70.

[38] Itani, H., Saad, G., &Chehab, G. (2016). The use of geogrid reinforcement for enhancing the performance of concrete overlays: An experimental and numerical assessment. *Construction and Building Materials*, *124*, 826-837. https://doi.org/10.1016/j.conbuildmat.2016.08.013

[39] Al Azzawi, A. A. (2012). Finite element analysis of flexible pavements strengthed with geogrid. *ARPN Journal of Engineering and Applied Sciences*, *7*(10), 1295-1299.

[40] Correia, N. S., Esquivel, E. R., & Zornberg, J. G. (2018). Finite-Element Evaluations of Geogrid-Reinforced Asphalt Overlays over Flexible Pavements. J. *Transp. Eng., Part B: Pavements*, *144*(2). https://doi:10.1061/JPEODX.0000043

[41] Rahman, M. M., Saha, S., A. S. A., Hamdi, A. S. A., & Bin Alam, M. J. (2019). Development of 3-D Finite Element Models for Geo-Jute Reinforced Flexible Pavement. *Civil Engineering Journal*, *5*(2), 437-446. http://doi.org/10.28991/cej-2019-03091258

[42] Abu El Maaty, A. E. (2017). Temperature Change Implications for Flexible Pavement Performance and Life. *International Journal of Transportation Engineering and Technology*, *3*(1), 1-11. https://doi:10.11648/j.ijtet.20170301.11

[43] Hadi, M. N. S. & Bodhinayake, B. C. (2003). Non-linear finite element analysis of flexible pavementsz. *Advances in Engineering Software*, *34*, 657-662. https://doi:10.1016/S0965-9978(03)00109-1

[44] Chang, D. T. T., Ho, N. H., Yi, C. H., & Yeh, H. S. (1999). Laboratory and Case Study for Geogrid-Reinforced Flexible Pavement Overlay. *Transportation Research Board*, *1687*(1), 125-130. https://doi.org/10.3141/1687-14

[45] Akrma, H. A, Hilal, M. M., & Fattah, M. Y. (2022). Numerical Simulation of the Effect of Repeated Load and Temperature on the Behavior of Asphalt Layers. *Engineering and Technology Journal*, *40*(05), 1-10. http://doi.org/10.30684/etj.v40i5.1012

Contact informations:

Abdelkader MEDJDOUB, PhD Student
Geomaterials and Civil Engineering Laboratory,
Civil Engineering Department,
University of Blida 1,
Soumaa Road, N°270, Blida, Algeria
E-mail: abdelmejd@yahoo.fr

Mouloud ABDESSEMED, Senior Lecturer, PhD
(Corresponding author)
Geomaterials and Civil Engineering Laboratory,
Civil Engineering Department,
University of Blida1,
Soumaa Road, N°270, Blida, Algeria
E-mail: abdesmoul@yahoo.fr